Giant Magnetoresistance in Heterogeneous Cu-Co Alloys

A. E. Berkowitz,[1,2] J. R. Mitchell,[1,2] M. J. Carey,[1,2] A. P. Young,[1,2] S. Zhang,[3] F. E. Spada,[2] F. T. Parker,[2] A. Hutten,[4] and G. Thomas[4]

[1]*Department of Physics, University of California at San Diego, La Jolla, California 92093*

[2]*Center for Magnetic Recording Research, University of California at San Diego, La Jolla, California 92093*

[3]*Department of Physics, New York University, 4 Washington Place, New York, New York 10003*

[4]*Department of Materials Science and Mineral Engineering and National Center for Electron Microscopy, Lawrence Berkeley Laboratory, University of California at Berkeley, Berkeley, California 94720*

(Received 20 February 1992)

We have observed giant magnetoresistance in heterogeneous thin film Cu-Co alloys consisting of ultrafine Co-rich precipitate particles in a Cu-rich matrix. The magnetoresistance scales inversely with the average particle diameter. This behavior is modeled by including spin-dependent scattering at the interfaces between the particles and the matrix, as well as the spin-dependent scattering in the Co-rich particles.

PACS numbers: 72.15.Gd, 72.15.He, 75.50.Rr, 75.60.Jp

The recent reports of giant magnetoresistance (GMR) in a number of antiferromagnetically coupled multilayer systems [1-3] have stimulated widespread research activity. Modeling of the GMR has emphasized spin-dependent scattering both within the ferromagnetic layer and at the interfacial region between the ferromagnetic and nonferromagnetic layers [4,5]. The GMR phenomenon is different from the conventional MR which is due to the effect of magnetic fields acting directly on the conduction electrons or on the scattering impurities. The GMR in multilayered structures comes from the reorientation of the single domain magnetic layers. This is the reason GMR is not usually seen in conventional bulk magnetic materials. GMR is observed in both antiferromagnetically coupled and uncoupled layer structures, as a consequence of the fact that the relative orientation of the magnetization of successive ferromagnetic layers changes from antiparallel to parallel in an applied field. For systems with uncoupled magnetic layers, the orientation of the magnetization is random at the coercive magnetic field (H_c) and there are many magnetic layers which are statistically arranged antiparallel. If these uncoupled layers are replaced by single domain magnetic particles in a nonmagnetic matrix, one should also expect GMR. Our objective was to produce an alloy with a significant volume fraction of magnetic particles, and to demonstrate that GMR is not restricted to multilayered systems. In this Letter, we report that in one such alloy, Cu-Co, GMR is clearly observed.

Cu-Co is an obvious choice since the largest MR changes have been reported for this multilayer system [6]. In addition, the generally accepted equilibrium phase diagram [7] shows virtually no solubility of Co in Cu, and <9 at.% solubility of Cu in Co, below 500 °C. A more recent phase diagram [8] indicates essentially no solubility of Cu in Co. Thus we expect, at equilibrium, a mixture of Cu and Co phases. Kneller [9] showed many years ago that Cu-Co films evaporated at room temperature formed metastable fcc solid solutions which dissociated into the equilibrium phases upon annealing. Recently, Childress and Chien [10,11] prepared Cu-Co films by sputtering onto liquid-N_2-cooled substrates. They found evidence from susceptibility data for both pure and reentrant spin-glass behavior in the as-deposited films. They reported coercive forces on annealing as high as 600 Oe, which they suggested indicate the presence of ultrafine Co-rich precipitates in a Cu-rich matrix [11]. We prepared Co-Cu films by dc magnetron sputtering from separate Cu and Co targets onto Si(100) substrates at room temperature. The substrates rotated above the targets at 1 revolution/s. The background pressure was 6×10^{-7} torr. Sputter rates were adjusted to yield films of three compositions: 12, 19, and 28 at.% Co (12 Co, 19 Co, and 28 Co). The films were 3000 Å thick. Samples were examined as-deposited and after annealing in flowing H_2 or He-5% H_2. Characterization techniques were x-ray and electron diffraction, transmission electron microscopy (TEM), vibrating-sample and superconducting quantum interference device magnetometry, and four-point probe MR. The samples for TEM were 500 Å thick, deposited onto 300-Å Si-N electron transparent grids.

Details of the structural, magnetic, and transport properties will be published separately. This Letter focuses on the GMR, and only the principal features of the general properties will be noted. Our samples' magnetic and structural properties were similar to those reported by Childress and Chien [10,11] with one exception. Our as-deposited 19 Co and 28 Co samples did not exhibit sharp maxima in susceptibility versus temperature, but rather broad peaks after zero-field cooling and no maximum after field cooling, as shown in Fig. 1. Our higher substrate temperatures very likely produced an increased chemical short-range order, i.e., Co-rich clusters. Some evidence for such clusters was provided by x-ray diffraction spectra of the 19 Co and 28 Co as-deposited

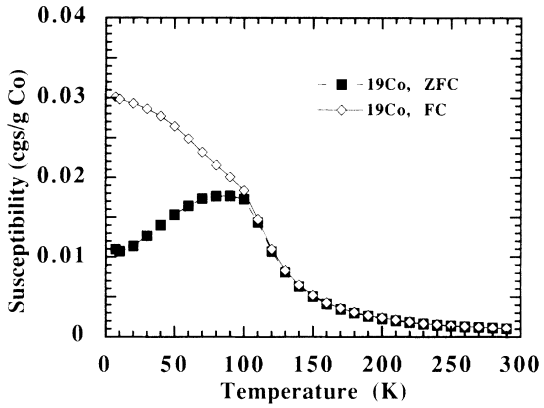

FIG. 1. Temperature dependence of dc susceptibility of the as-deposited 19 Co film in 10 Oe applied field. ZFC represents zero-field cooled; FC represents field cooled.

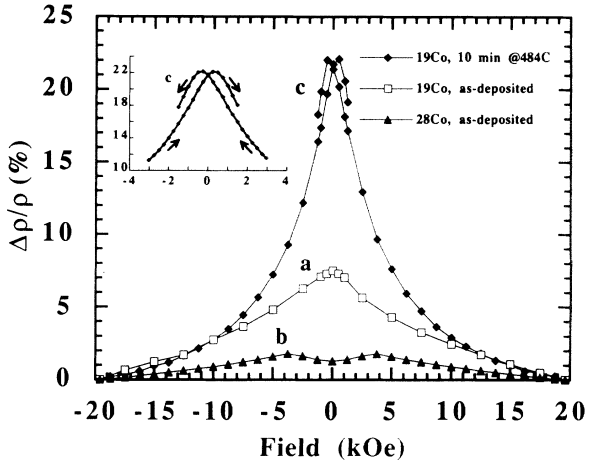

FIG. 2. Field dependence of $\Delta\rho/\rho = (\rho_{H_c} - \rho_{H=20\,\mathrm{kOe}})/\rho_{H=20\,\mathrm{kOe}}$ for the three types of curves obtained. Inset: Details of curve *c*. Curves *a* and *b* measured at $T = 100$ K; curve *c* measured at 10 K. Sense current parallel to field.

samples. A single fcc phase was measured but a slight asymmetry in the 220 peak was consistent with the presence of a small fraction of fcc Co clusters. Thus Fig. 1 reflects the distribution of blocking temperatures of those superparamagnetic clusters [12]. The isothermal remanence at 10 K was only a few percent of saturation for the 19 Co and 28 Co as-deposited samples. Thus the Co-rich clusters constituted only a small fraction of the Co atoms. However, the susceptibility versus temperature behavior of these clusters (Fig. 1) could have masked the sharp susceptibility maxima at low temperatures reported by Childress and Chien [10] for the fcc Cu-Co matrix phase. The MR curves for the as-deposited 12 Co sample at $T > 10$ K and for the as-deposited 19 Co at $T \geq 100$ K suggested a paramagnetic state as shown in Fig. 2, curve *a*, for 19 Co. The shapes of the MR curves for the as-deposited 28 Co sample at $T \leq 296$ K and the as-deposited 19 Co sample at 10 K were similar to the example shown in Fig. 2, curve *b*. A plausible explanation for the as-deposited samples' behavior is as follows: The 12 Co sample was single phase disordered fcc with the spin-glass-like susceptibility behavior described by Childress and Chien [10]. The 19 Co and 28 Co samples had a small fraction of Co-rich superparamagnetic clusters with average blocking temperatures of ~100 K (19 Co) and ~350 K (28 Co). The major fractions of the 19 Co and 28 Co samples were disordered fcc alloys. The minimum in MR in Fig. 2, curve *b* suggests domainlike regions which are saturated in relatively low fields. The as-deposited 28 Co samples had this MR shape at all measured temperatures and the resistivity maxima occurred at the knee of the magnetization curves, i.e., where the "domains" were aligned. All three as-deposited samples were in the composition region in which Kneller [9] found no spin moment, and Childress and Chien's [10] data and ours suggested a breakdown of magnetic order; i.e., the samples at $T < 10$ K do not saturate in 50 kOe. Thus the weak exchange among the nonpercolating Co atoms competes with the anisotropy energy to produce a spin-glass state or, more likely in our samples, a mixture of clusters in a matrix of a disordered fcc Cu-Co alloy [13].

Although the as-deposited samples such as 19 Co show GMR as large as 10% at 10 K, the MR is negligible at room temperature. We note that the resistivity of the as-deposited samples is as high as 50 $\mu\Omega$ cm due to their highly disordered state and fine grain size. We, therefore, annealed the samples to reduce the temperature dependence of the GMR and to obtain larger MR. Upon annealing, in addition to grain size increase, phase separation between Co and Cu occurs and stable Co particles are formed. These factors substantially reduce the disorder as compared to the as-deposited state; the resistivity drops to ~5–10 $\mu\Omega$ cm, depending on the annealing times and temperatures. After annealing, the 19 Co and 28 Co samples showed the largest MR changes. Their MR curves had the shape shown in Fig. 2, curve *c*. The maximum MR occurred at the coercive force H_c which was ~500 Oe at 10 K for all annealed 19 Co and 28 Co samples. Remanence/saturation (M_R/M_S) ratios were > 0.3 at 10 K for all annealed samples. Both H_c and M_R/M_S decreased with increasing measuring temperature and annealing time. The magnetic behavior of the annealed samples was associated with the precipitation of Co-rich particles in a Cu-rich matrix. Figure 3 shows a transmission electron micrograph of the 19 Co sample after annealing 10 min at 484 °C. The Co-rich precipitates can be identified by the diffraction and interference-induced contrast changes in small regions [14]. These precipitates have an ~40 Å average diameter with an average spacing of ~80 Å. The sample shown in Fig. 3 had the largest MR observed. Figure 4 shows $\Delta\rho/\rho$ vs T for as-deposited and annealed 19 Co and 28 Co speci-

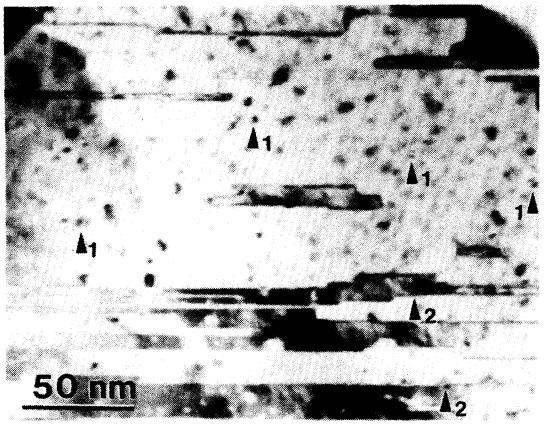

FIG. 3. Bright-field micrograph of 19 Co sample annealed for 10 min at 484 °C. Co particles labeled 1 show typical Ashby-Brown [14] strain field contrast of spherical precipitates. The contrast of particles labeled 2 is due to moiré contrast.

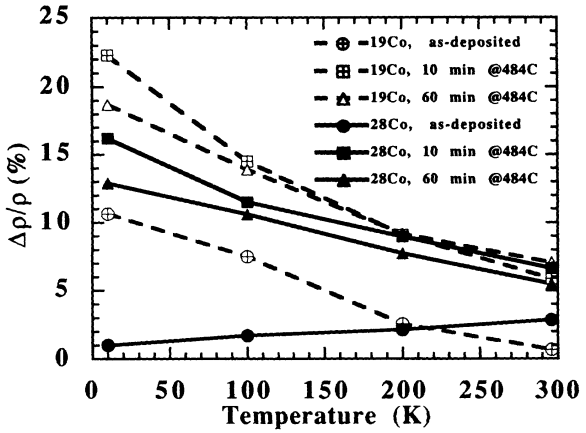

FIG. 4. Temperature dependence of $\Delta\rho/\rho$ for 19 Co and 28 Co samples treated as indicated.

mens. Saturation fields for the MR coincided with the saturation fields for the magnetization. The MR ratio increased with decreasing annealing temperature and time (except for the as-deposited 28 Co). The data clearly indicated a giant MR in the annealed samples associated with the presence of appropriately sized and spaced Co-rich precipitate particles.

As annealing times and temperatures increased, the average Co-rich particle sizes also increased, with the corresponding decrease in MR noted above. Larger Co particles have several adverse effects on MR. The surface/volume ratio decreases, which reduces the spin-dependent interfacial scattering relative to bulk scattering processes. This effect is considered below. Furthermore, the particles will become larger than the mean free path within the particles. Finally, when the particles are no longer single domains, the interaction of the conduction electron spins with the varying magnetization distribution in the particles produces a state in which the conduction electron spin channels are mixed. This will reduce the MR. On the other hand, Co particles that are too small will be subject to thermally activated magnetization reversal, i.e., superparamagnetism. Superparamagnetism in the as-deposited 19 Co sample is very likely responsible for the enormous temperature dependence of $\Delta\rho/\rho$ seen in Fig. 4. The annealed samples have MR temperature dependences similar to those found in GMR multilayers [6].

The GMR in these heterogeneous Cu-Co alloys may be analyzed in the same manner as in Cu-Co multilayers. We assume a random distribution of Co particles with average radius r_{Co}, in a Cu matrix, and adopt a spin-dependent scattering model at the surface of Co particles and within the Co particles. The conductivity can be written as [15]

$$\sigma = \frac{ne^2}{2m}\sum_{\sigma}\frac{1}{\Delta^{\sigma}}, \tag{1}$$

where Δ^{σ} is the average scattering matrix. The phenomenological input for Δ^{σ} is

$$\Delta^{\sigma} = \Delta_{Cu} + \Delta^{g}_{Co} + \Delta^{g}_{S}, \tag{2}$$

where

$$\Delta_{Cu} \propto (1-c)/\lambda_{Cu},$$

$$\Delta^{g}_{Co} \propto \frac{c}{\lambda_{Co}}(1 + p^2_{Co} + 2p_{Co}\hat{\sigma}\cdot\hat{\mathbf{M}}_{Co}),$$

$$\Delta^{g}_{S} \propto \frac{3c\xi}{r_{Co}}(1 + p^2_{S} + 2p_{S}\hat{\sigma}\cdot\hat{\mathbf{M}}_{Co}),$$

and c is the Co concentration; λ_{Cu} and λ_{Co} are the mean free paths of Cu and Co, respectively; ξ is the scattering strength for surfaces; p_{Co} and p_S are the spin-dependent ratios for scattering within the Co particles and at their surfaces, respectively. Thus Eq. (1) is the sum of scattering in Cu, Co, and at the interfaces between them. Since

$$\Phi = \frac{\sigma(H=H_s) - \sigma(H=H_c)}{\sigma(H=H_c)}, \tag{3}$$

we now substitute Eq. (2) into Eq. (1), and Eq. (3) becomes

$$\Phi = \frac{\sigma^{\uparrow}(H=H_S) + \sigma^{\downarrow}(H=H_S) - 2\sigma(H=H_c)}{2\sigma(H=H_c)}, \tag{4}$$

where

$$\sigma^{\downarrow\uparrow}(H=H_S) = \left[\frac{1-c}{\lambda_{Cu}} + \frac{c}{\lambda_{Co}}(1\pm p_{Co})^2 + \frac{3c\xi}{r_{Co}}(1\pm p_S)^2\right]^{-1},$$

with $\pm$ referring to spin up and down, and

$$\sigma(H=H_c)=\left[\frac{1-c}{\lambda_{Cu}}+\frac{c}{\lambda_{Co}}(1+p_{Co}^2)+\frac{3c\xi}{r_{Co}}(1+p_S^2)\right]^{-1}.$$

In Co/Cu multilayers, the principal spin-dependent scattering is from the interfacial term ($p_S=0.5$, $p_{Co}=0.2$, $\xi=0.3$) [16]. Thus, if we take $p_{Co}\approx 0$, Eq. (4) reduces to

$$\Phi\approx\frac{4p_S^2}{(1-p_S^2)^2+2\alpha(1+p_S^2)r_{Co}+\alpha^2 r_{Co}^2}, \quad (5)$$

where

$$\alpha\equiv\frac{(1-c)/\lambda_{Cu}+c/\lambda_{Co}}{3c\xi}.$$

Equation (5) correctly predicts the inverse dependence of MR on the particle size, in accordance with the surface/volume ratio consideration noted above. In order to obtain better than an order of magnitude estimate of the agreement of the predictions of Eq. (5) with our measurements, we need reliable estimates of some of the parameters, particularly λ_{Cu} and λ_{Co}. This requires detailed data on the compositions and ρ's of the Co-rich particles and Cu-rich matrix. Experiments to obtain this information are in progress.

Thus, we have shown that GMR is not restricted to multilayer structures, but is also found in suitable heterogeneous alloy systems consisting of single domain particles in a nonmagnetic (or weakly magnetic) matrix. These results open a new range of systems for testing GMR models, as well as providing additional opportunities for technological applications.

We appreciate discussions with M. B. Maple and assistance with high-field MR measurements by M. C. de Andrade. This work was partially supported by NSF Grant No. DMR-90-10908, and by ONR Grant No. N00014-91-J-1695.

[1] M. N. Baibich, J. M. Broto, A. Fert, F. Nguyen van Dau, F. Petroff, P. Etienne, G. Creuzet, A. Friedrich, and J. Chazelas, Phys. Rev. Lett. **61**, 2472 (1988).
[2] S. S. P. Parkin, N. More, and K. P. Roche, Phys. Rev. Lett. **64**, 2304 (1990).
[3] W. P. Pratt, Jr., S.-F. Lee, J. M. Slaughter, R. Loloee, P. A. Schroeder, and J. Bass, Phys. Rev. Lett. **66**, 3060 (1991), and references therein.
[4] P. M. Levy, S. Zhang, and A. Fert, Phys. Rev. Lett. **65**, 1643 (1990).
[5] R. E. Camley and J. Barnas, Phys. Rev. Lett. **63**, 664 (1989).
[6] S. S. P. Parkin, Z. G. Li, and D. J. Smith, Appl. Phys. Lett. **58**, 2710 (1991).
[7] M. Hansen, *Constitution of Binary Alloys* (McGraw-Hill, New York, 1958), p. 469.
[8] T. Nishizawa and K. Ishida, Bull. Alloy Phase Diagrams **5**, 161 (1984).
[9] E. Kneller, J. Appl. Phys. **33S**, 1355 (1962).
[10] J. R. Childress and C. L. Chien, Phys. Rev. B **43**, 8089 (1991).
[11] J. R. Childress and C. L. Chien, J. Appl. Phys. **70**, 5885 (1991).
[12] L. Néel, Adv. Phys. **4**, 191 (1955).
[13] S. Crane, D. W. Carnegie, Jr., and H. Claus, J. Appl. Phys. **53**, 2179 (1982).
[14] M. F. Ashby and L. M. Brown, Philos. Mag. **8**, 1083 (1963).
[15] S. Zhang and P. M. Levy, J. Appl. Phys. **69**, 4768 (1991).
[16] S. Zhang and P. M. Levy, in *Magnetic Thin Films, Multilayers and Surfaces*, edited by S. S. P. Parkin *et al.*, MRS Symposia Proceedings No. 231 (Materials Research Society, Pittsburgh, 1991), p. 255.

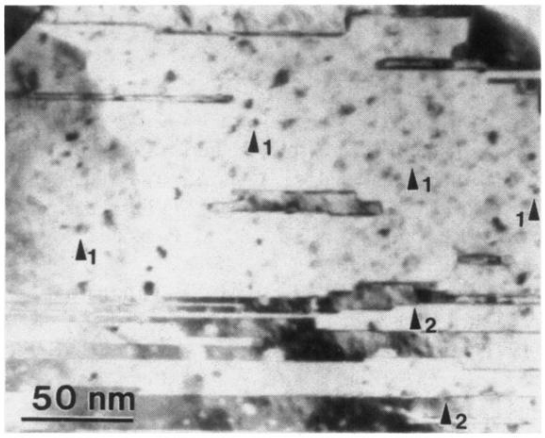

FIG. 3. Bright-field micrograph of 19 Co sample annealed for 10 min at 484 °C. Co particles labeled 1 show typical Ashby-Brown [14] strain field contrast of spherical precipitates. The contrast of particles labeled 2 is due to moiré contrast.